

Non-Antipodal Signaling based Semi-Blind Detector in Uplink Cell-Free mMIMO Networks

N V Divya Lakshmi, Adarsh Patel

School of Computing and Electrical Engineering (SCEE), Indian Institute of Technology Mandi, Mandi, India

Email: S22007@students.iitmandi.ac.in, adarsh@iitmandi.ac.in

Abstract—This work presents a novel data detection algorithm for uplink Cell-Free Massive Multiple-Input Multiple-Output (CF-mMIMO) networks that operates without pilot transmission overhead. In the proposed framework, User Equipments (UEs) transmit non-antipodal signals to a Central Processing Unit (CPU), which jointly processes the composite received signals to recover user information. An Alternating Least Squares (ALS)-based Non-Antipodal Signaling Semi-Blind (NASS) detection algorithm is developed to enable pilot-free data detection in TDD uplink CF-mMIMO systems. The proposed algorithm exploits the inherent tensor structure of the received signal to extend the conventional ALS framework, effectively resolving permutation and scaling ambiguities for accurate semi-blind detection. Simulation results demonstrate that the NASS detector achieves significantly improved Bit Error Rate (BER) performance compared to existing iterative and pilot-assisted algorithms, confirming its robustness, scalability, and practical suitability for next-generation ISAC and CF-mMIMO deployments.

Index Terms—Cell-free massive MIMO (CF-mMIMO), Non-antipodal Signaling, semi-blind detection, Alternating Least Squares (ALS).

I. INTRODUCTION

Cell-Free Massive Multiple-Input Multiple-Output (CF-mMIMO) is an emerging 6G technology that integrates the advantages of distributed antenna systems and massive MIMO architectures to achieve ubiquitous coverage, uniform Quality of Service, and improved energy efficiency [1]. In a CF-mMIMO network, a large number of geographically distributed Access Points (APs) are connected to a Central Processing Unit (CPU) via fronthaul links, collaboratively serving multiple User Equipments (UEs) across the coverage area [2]. In the uplink, the APs forward the received signals to the CPU, which performs joint signal detection and data processing, thereby mitigating inter-user interference and enhancing overall system performance.

Data detection in CF-mMIMO systems fundamentally relies on accurate Channel State Information (CSI), which is conventionally obtained through pilot symbol transmission. However, in CF-mMIMO scenarios, pilot-based channel estimation introduces a significant communication overhead due to the large number of APs and UEs. Moreover, in dense UE deployments, performing centralized data decoding at the CPU demands high fronthaul bandwidth, leading to scalability and latency challenges. To address these limitations, decentralized architectures have been explored in recent works [3], [4], where each AP processes its local observations and exchanges soft information with neighboring APs. While this

approach effectively reduces the CPU's computational load, it introduces frequent inter-AP communication and requires tight fronthaul coordination. Other works [5], [6] assume perfect knowledge of large scale fading coefficients, which limits their applicability to practical deployments. Nonetheless, these methods still depend on pilot transmission, thereby sustaining a non-negligible overhead.

In parallel, several tensor decomposition-based joint channel estimation and data detection techniques have been proposed [7]–[10], though primarily for systems other than CF-mMIMO. Motivated by these gaps, this work proposes a novel Non-Antipodal Signaling based Semi-Blind (NASS) detection algorithm that eliminates the need for pilot transmission in TDD uplink CF-mMIMO networks, offering improved efficiency and scalability for practical large-scale deployments.

The next Section II presents the uplink CF-mMIMO system model. Section III presents the framework to obtain the proposed NASS detection algorithm. Section IV evaluates the performance of the proposed detection algorithm with the baseline, pilot-assisted, and iterative detectors. Finally, Section V presents the conclusion and future scope of this work. Scalars, vectors, matrices and tensors are represented by italic, boldface lowercase, bold uppercase and boldface calligraphic letters, respectively. The operators $\|\cdot\|_F$, $(\cdot)^T$, $(\cdot)^H$, $(\cdot)^{-1}$, $(\cdot)^\dagger$, \circ , \odot denotes Frobenius norm, transpose, hermitian transpose, inverse, pseudo-inverse, outer product and Khatri-Rao product operations [11], respectively.

II. SYSTEM MODEL

Consider an uplink CF-mMIMO system with R single antenna APs connected to a CPU serving U single antenna UEs, $R \gg U$. The element g_{ru} of the uplink channel vector $\mathbf{g}_u \in \mathbb{C}^{R \times 1}$ between UE u , $1 \leq u \leq U$, and R APs follows a complex Normal distribution, i.e., $g_{ru} \sim \mathcal{CN}(0, \beta_{ru})$ where β_{ru} is the large-scale fading coefficient between AP r and UE u . The vector $\mathbf{d}_u \in \mathbb{R}^{K \times 1}$ be the data of UE u where each non-antipodal element $d_{ru} \in \{0, \sqrt{2}\}$ is encoded with orthogonal code $\mathbf{s}_u \in \mathbb{R}^{L \times 1}$ as $\mathbf{d}_u \circ \mathbf{s}_u = \mathbf{d}_u \mathbf{s}_u^T \in \mathbb{R}^{K \times L}$. The non-antipodal/ on-off signaling convey different meanings across applications - in radar systems, it denotes the presence or absence of a target; in backscatter communication, the reflection or absorption of an incident wave; in wireless sensing networks and IoT applications, the occurrence or non-occurrence of a physical event, etc., and across these applications works with noncoherent low complexity energy

detector. The APs are connected to the CPU via error-free front-haul links. The composite signal tensor $\mathcal{Y} \in \mathbb{C}^{K \times L \times R}$ received at CPU from R APs corresponding to U UEs, each transmitting K symbols, in uplink CF-mMIMO networks is

$$\mathcal{Y} = \sum_{u=1}^U \mathbf{d}_u \circ \mathbf{s}_u \circ \mathbf{g}_u + \mathcal{N} = \mathbf{D} \circ \mathbf{S} \circ \mathbf{G} + \mathcal{N}, \quad (1)$$

where the element $n_{klr} \sim \mathcal{CN}(0, \sigma_n^2)$ of the noise tensor $\mathcal{N} \in \mathbb{C}^{K \times L \times R}$ follows complex Normal distribution. Column u of the data matrix $\mathbf{D} = [\mathbf{d}_1 \dots \mathbf{d}_u \dots \mathbf{d}_U] \in \mathbb{R}^{K \times U}$ and the code matrix $\mathbf{S} = [\mathbf{s}_1 \dots \mathbf{s}_u \dots \mathbf{s}_U] \in \mathbb{R}^{L \times U}$ denote the data and code of user u . The channel coefficient matrix is $\mathbf{G} = [\mathbf{g}_1 \dots \mathbf{g}_u \dots \mathbf{g}_U] \in \mathbb{C}^{R \times U}$. The received signal \mathcal{Y} , a 3rd order tensor, in (1) is presented as the sum of unit rank tensors, where the u th unit rank tensor $\mathbf{d}_u \circ \mathbf{s}_u \circ \mathbf{g}_u$ is obtained from the outer product of the u th column vectors of the corresponding matrices \mathbf{D} , \mathbf{S} and \mathbf{G} for $1 \leq u \leq U$. Next section presents the pilot-less detection algorithm in uplink CF-mMIMO systems.

III. NON-ANTIPODAL SIGNALING BASED SEMI-BLIND (NASS) DETECTOR

The objective to detect the UE signal \mathbf{D} from composite received tensor \mathcal{Y} in (1) without pilot transmission overhead

$$\mathcal{L}(\hat{\mathbf{D}}, \hat{\mathbf{G}}) = \min_{\mathbf{D}, \mathbf{G}} \|\mathcal{Y} - \mathbf{D} \circ \mathbf{S} \circ \mathbf{G}\|_F^2, \quad (2)$$

where $\hat{\mathbf{D}}$ and $\hat{\mathbf{G}}$ denotes the reconstructed versions of factor matrices \mathbf{D} and \mathbf{G} . The bilinear multi-objective cost function (2) is simplified by alternately optimizing one factor matrix while keeping the others fixed, known as alternating least squares (ALS). Using the mode- r matricization [11], unfoldings of system model (1) along mode-3 and mode-1 be

$$\mathbf{Y}_{(3)} = \tilde{\mathbf{G}}^{(i)} (\mathbf{S} \odot \tilde{\mathbf{D}}^{(i-1)})^T + \mathbf{N}_{(3)} \quad (3)$$

$$\mathbf{Y}_{(1)} = \tilde{\mathbf{D}}^{(i)} (\tilde{\mathbf{G}}^{(i)} \odot \mathbf{S})^T + \mathbf{N}_{(1)} \quad (4)$$

The matrices $\mathbf{Y}_{(3)}/\mathbf{N}_{(3)}$ is mode-3 unfolding and $\mathbf{Y}_{(1)}/\mathbf{N}_{(1)}$ mode-1 unfolding of the tensor \mathcal{Y}/\mathcal{N} . The non-linear objective $\mathcal{L}(\hat{\mathbf{D}}, \hat{\mathbf{G}})$ in (2) to its equivalent linear least-square (LS) objectives to get $\hat{\mathbf{G}}^{(i)}$ and $\hat{\mathbf{D}}^{(i)}$ without sending pilots are

$$\hat{\mathbf{G}}^{(i)} = \arg \min_{\mathbf{G}^{(i)}} \left\| \mathbf{Y}_{(3)} - \mathbf{G}^{(i)} (\mathbf{S} \odot \tilde{\mathbf{D}}^{(i-1)})^T \right\|_F^2 \quad (5)$$

$$\tilde{\mathbf{D}}^{(i)} = \arg \min_{\mathbf{D}^{(i)}} \left\| \mathbf{Y}_{(1)} - \mathbf{D}^{(i)} (\tilde{\mathbf{G}}^{(i)} \odot \mathbf{S})^T \right\|_F^2. \quad (6)$$

$\mathbf{A}^{(i)}$ is an intermediate updated matrix \mathbf{A} at iteration i and tilde notation ($\tilde{\mathbf{G}}^{(i)}/\tilde{\mathbf{D}}^{(i)}$) denotes the error due to the linear simplification of the non-linear cost (2). The cost functions in (5), (6) have closed form solutions, given as

$$\tilde{\mathbf{G}}^{(i)} = \mathbf{Y}_{(3)} \left[(\mathbf{S} \odot \tilde{\mathbf{D}}^{(i-1)})^T \right]^\dagger \quad (7)$$

$$\tilde{\mathbf{D}}^{(i)} = \mathbf{Y}_{(1)} \left[(\tilde{\mathbf{G}}^{(i)} \odot \mathbf{S})^T \right]^\dagger. \quad (8)$$

The channel matrix $\tilde{\mathbf{G}}^{(i)}$ in (7) and data matrix $\tilde{\mathbf{D}}^{(i)}$ in (8) are updated alternately (ALS) to equivalently solve the non-linear cost $\mathcal{L}(\hat{\mathbf{D}}, \hat{\mathbf{G}})$ in (2). However, due to permutation and

scaling ambiguities [11], ALS algorithm does not guarantee correct solution. The proposed NASS detection in Algorithm 1 resolves permutation ambiguity by aligning columns of $\tilde{\mathbf{G}}^{(i)}$ and $\tilde{\mathbf{D}}^{(i)}$ with the known code matrix \mathbf{S} . The scaling ambiguity is resolved by fixing the sign of 1st data bit of all UEs as reference, i.e., $\tilde{\mathbf{D}}^{(0)}(1, :) = \mathbf{1}^T \in \mathbb{R}^{1 \times U}$. The diagonal scaling matrix $\mathbf{\Lambda}^{(i)}$ is obtained from the first row $\tilde{\mathbf{D}}^{(0)}(1, :)$ as where the operator $\text{diag}(\mathbf{k})$ constructs a diagonal matrix whose principal diagonal entries correspond to the elements of the vector \mathbf{k} . Consequently, $\mathbf{\Lambda}^{(i)}$ is a diagonal matrix that represents the scaling factors associated with each UE's data during iteration i . This process of sending a sign bit per user may be seen as equivalent to sending a pilot symbol overhead. However, unlike conventional pilot-assisted transmission, the overhead incurred by this operation is fixed and independent of the number of APs or UEs, thereby ensuring scalability and efficiency in large-scale CF-mMIMO deployments. The scaling deviation is then corrected by scaling and counter-scaling the respective columns of $\tilde{\mathbf{G}}^{(i)}$ and $\tilde{\mathbf{D}}^{(i)}$ as

$$\hat{\mathbf{D}}^{(i)} \circ \mathbf{S} \circ \hat{\mathbf{G}}^{(i)} = \tilde{\mathbf{D}}^{(i)} \left(\mathbf{\Lambda}^{(i)} \right)^{-1} \circ \mathbf{S} \circ \tilde{\mathbf{G}}^{(i)} \left(\mathbf{\Lambda}^{(i)} \right). \quad (9)$$

The NASS algorithm terminates when error $E^{(i)}$, defined as

$$E^{(i)} = \|\mathbf{Y}_{(1)} - \hat{\mathbf{D}}^{(i)} (\hat{\mathbf{G}}^{(i)} \odot \mathbf{S})^T\|_F^2, \quad (10)$$

is below a tolerance level ϵ [11] or the iteration i attains I . The steps to obtain the NASS detector in the uplink CF-mMIMO networks is given in Algorithm 1. Next section demonstrates the effectiveness of the NASS detector via simulations.

IV. SIMULATION RESULTS

Consider an uplink CF-mMIMO network with $R = 64$ APs, $U = 8$ users uniformly distributed over a 100m² area, Large-scale fading coefficient β_{ru} modeled as $\beta_{ru} = \min\{1, d_{ru}^{-\alpha}\}$, where d_{ru} is the distance between AP r and UE u for path-loss exponent $\alpha = 1$ [13]. The algorithm is prematurely halted when the iteration index i attains the predefined maximum of $I = 12$ or if the error tolerance $\epsilon = 10^{-3}$ is satisfied [14].

Algorithm 1: NASS Detection in uplink CF-mMIMO

Data: mode-1 and mode-3 unfoldings $\mathbf{Y}_{(1)}$ and $\mathbf{Y}_{(3)}$ of tensor $\mathcal{Y} \in \mathbb{C}^{K \times L \times R}$ and the code matrix \mathbf{S}

Result: Data matrix $\hat{\mathbf{D}}_{NASS}$

- 1 $\hat{\mathbf{D}}^{(0)}(1, :) = \mathbf{1}^T \leftarrow$ Initializing the sign bit of users
 - 2 **repeat**
 - 3 $\tilde{\mathbf{G}}^{(i)} \leftarrow$ Update channel matrix from (7)
 - 4 $\tilde{\mathbf{D}}^{(i)} \leftarrow$ Update data matrix from (8)
 - 5 $\mathbf{\Lambda}^{(i)} \leftarrow \text{diag}(\tilde{\mathbf{D}}^{(i)}(1, :))$; // get scaling matrix
 - 6 $\hat{\mathbf{D}}^{(i)} \leftarrow \tilde{\mathbf{D}}^{(i)} (\mathbf{\Lambda}^{(i)})^{-1}$; // scaling from (9)
 - 7 $\hat{\mathbf{G}}^{(i)} \leftarrow \tilde{\mathbf{G}}^{(i)} \mathbf{\Lambda}^{(i)}$; // counter-scaling from (9)
 - 8 $i \leftarrow i + 1$
 - 9 **until** ($E^{(i)} > \epsilon$ or $i < I$);
 - 10 **return** Data matrix $\hat{\mathbf{D}}_{NASS} = \hat{\mathbf{D}}^{(i)}$.
-

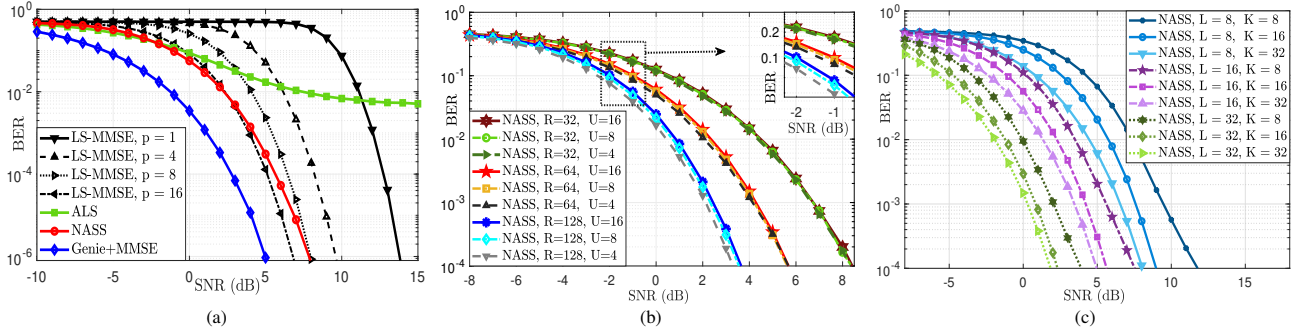


Fig. 1: BER vs. SNR performance of proposed NASS (Algorithm 1) in uplink CF-mMIMO for (a) Data and Code lengths $K = L = 16$, $R = 64$ APs, and $U = 8$ users with ALS [11], pilot-assisted LS-MMSE [12] with pilot symbols per user $p \in \{1, 4, 8, 16\}$, and perfect Channel-based Genie-MMSE; (b) a fixed $K = L = 16$, users $U \in \{4, 8, 16\}$ and APs $R \in \{32, 64, 128\}$; (c) a fixed $R = 64$ APs, $U = 8$, $K \in \{8, 16, 32\}$ and $L \in \{8, 16, 32\}$.

Fig. 1a presents BER vs. SNR comparisons of the proposed NASS algorithm in Section III with the with pilot-assisted LS channel estimator followed by MMSE detection (LS-MMSE) [12] with pilot lengths $p = \{1, 4, 8, 16\}$, the true CSI aware Genie-MMSE, and the iterative ALS algorithm [14] with $U = 8$ users. The figure illustrates a superior performance of the NASS detector over the ALS by addressing the ambiguities. Moreover, NASS with a known sign bit (equivalent to $p = 1$ pilot symbol) has a BER performance at 10^{-6} similar to that of the pilot assisted LS-MMSE detector when sending eight times ($p = 8$) more pilot symbols. Moreover, an increase in the number of users will force LS-MMSE use a higher p to attain a performance similar to NASS. This is mainly due to construct of the NASS detector which requires only a sign bit to resolve ambiguities.

Fig. 1b and Fig. 1c presents the NASS detector for varying numbers of APs $R \in \{32, 64, 128\}$, users $U \in \{4, 8, 16\}$, data length $K \in \{8, 16, 32\}$ and code length $L \in \{8, 16, 32\}$. Fig. 1b illustrates an improvement in the detection performance as R increases whereas interestingly the detection performance remains similar with an increase in U . Fig. 1c illustrates that a large K or L results in significant BER improvement across SNRs. It is worth noting from Fig. 1b and Fig. 1c that, unlike conventional pilot-assisted transmission, the one sign-bit overhead required by the proposed NASS detection algorithm is fixed and remains independent of the parameters R , U , K and L .

V. CONCLUSION AND FUTURE WORK

This work presented non-antipodal signaling based pilot-free detection in uplink CF-mMIMO systems. Simulation results demonstrated that the proposed NASS detector achieves superior detection performance compared to both iterative and pilot-assisted baseline detection methods. Closed form expressions for BER performance analysis can be carried out upon the findings of this work and further be extended for non-ideal fornthahul links. The non-antipodal or the on-off signaling based framework comes in handy with sensing problems where the presence or absence of the target is to be identified. Hence, this detection framework can be tailored to

perform Integrated Sensing and Communication in the Cell-free massive MIMO Communication networks.

REFERENCES

- [1] P. Liu, K. Luo, D. Chen, and T. Jiang, "Spectral Efficiency Analysis of Cell-Free Massive MIMO Systems With Zero-Forcing Detector," *IEEE Transactions on Wireless Communications*, vol. 19, no. 2, pp. 795–807, 2020.
- [2] H. Q. Ngo, A. Ashikhmin, H. Yang, E. G. Larsson, and T. L. Marzetta, "Cell-Free Massive MIMO Versus Small Cells," *IEEE Transactions on Wireless Communications*, vol. 16, no. 3, pp. 1834–1850, 2017.
- [3] A. Karataev, C. Forsch, and L. Cottatellucci, "Bilinear Expectation Propagation for Distributed Semi-Blind Joint Channel Estimation and Data Detection in Cell-Free Massive MIMO," *IEEE Open Journal of Signal Processing*, vol. 5, pp. 284–293, 2024.
- [4] Z. Zhao and D. Slock, "Decentralized Message-Passing for Semi-Blind Channel Estimation in Cell-Free Systems Based on Bethe Free Energy Optimization," in *2024 58th Asilomar Conference on Signals, Systems, and Computers*, pp. 1443–1447, 2024.
- [5] Z. Zhao and D. Slock, "Bilinear Hybrid Expectation Maximization and Expectation Propagation for Semi-Blind Channel Estimation," in *2024 32nd European Signal Processing Conference (EUSIPCO)*, pp. 2122–2126, 2024.
- [6] Z. Zhao and D. Slock, "Expectation Propagation based Analysis of Semi-Blind Channel Estimation in Cell-Free Systems," in *2024 IEEE 25th International Workshop on Signal Processing Advances in Wireless Communications (SPAWC)*, pp. 836–840, 2024.
- [7] L. Zhao, S. Li, J. Zhang, and X. Mu, "A parafac-based blind channel estimation and symbol detection scheme for massive MIMO systems," in *2018 International Conference on Cyber-Enabled Distributed Computing and Knowledge Discovery (CyberC)*, pp. 350–3503, IEEE, 2018.
- [8] A. L. de Almeida, G. Favier, and J. C. M. Mota, "PARAFAC-based unified tensor modeling for wireless communication systems with application to blind multiuser equalization," *Signal Processing*, vol. 87, no. 2, pp. 337–351, 2007. Tensor Signal Processing.
- [9] A. Deshwal and A. Patel, "Blind Distributed Detection in MIMO Networks," in *2024 16th International Conference on COMMunication Systems & NETWORKS (COMSNETS)*, pp. 433–435, 2024.
- [10] N. Sidiropoulos, G. Giannakis, and R. Bro, "Blind PARAFAC receivers for DS-CDMA systems," *IEEE Transactions on Signal Processing*, vol. 48, no. 3, pp. 810–823, 2000.
- [11] N. D. Sidiropoulos, L. De Lathauwer, X. Fu, K. Huang, E. E. Papalexakis, and C. Faloutsos, "Tensor Decomposition for Signal Processing and Machine Learning," *IEEE Transactions on Signal Processing*, vol. 65, no. 13, pp. 3551–3582, 2017.
- [12] S. Yang and L. Hanzo, "Fifty Years of MIMO Detection: The Road to Large-Scale MIMOs," *IEEE Communications Surveys & Tutorials*, vol. 17, no. 4, pp. 1941–1988, 2015.
- [13] Z. Chen and E. Björnson, "Channel Hardening and Favorable Propagation in Cell-Free Massive MIMO with Stochastic Geometry," *IEEE Transactions on Communications*, vol. 66, no. 11, pp. 5205–5219, 2018.
- [14] T. G. Kolda and B. W. Bader, "Tensor Decompositions and Applications," *SIAM review*, vol. 51, no. 3, pp. 455–500, 2009.